

## Chapter 10

Mirosław Cholewa<sup>1</sup>, Andrzej Posmyk<sup>2</sup>, Dawid Scelina<sup>3</sup>, Łukasz Bąk<sup>4\*</sup>

### PREPARATION OF THE CONTACT SURFACE WITH THE COMPOSITION NEAR-EUTECTIC SILUMINS EPOXY (ALSI11/EP)

**Abstract:** This article presents preparation of near-eutectic aluminum-silicon surface (AC-AlSi11) by anodic oxidation, which produces a porous oxide layer (Al<sub>2</sub>O<sub>3</sub>) substrate constituting the permanent adhesive connection with an epoxy composition. Documents influence of silicon educe in the form of unmodified alloy (AC-AlSi11) and modified (AC-AlSi11 + M) in the anodizing process, uniform structure and thickness of the oxide layer and the topography of the surface to improve adhesion of the resin to AlSi alloy. This paper also describes the influence of the oxidized surface position in relation to the negative electrode i to the coating. In assumption elements of the test spatial castings will change the distribution of the electric field h resulting in a heterogeneous structure of the coating. The effect of surface preparation by oxidation on the mechanical properties of the connection AlSi alloy-resin is also described. The motivation for this study was a new group of products - spatial skeleton castings in which by regulation and prediction of effects at the border of the contact between ceramic and casting has influenced on structural and mechanical properties of cast skeleton composites.

**Key words:** oxidation, skeleton casting, adhesive connection

#### 10.1. Introduction

Ever-increasing demand for materials characterized by a low density while maintaining the mechanical properties similar to metal has lead to

---

<sup>1</sup>dr hab. inż., Silesian University of Technology, Faculty of Mechanical Engineering, Foundry Department, miroslaw.cholewa@polsl.pl

<sup>2</sup>dr hab. Andrzej Posmyk, Faculty of Transport, Silesian University of Technology, Department of Automotive Vehicle Service andrzej.posmyk@polsl.pl

<sup>3</sup>mgr inż., Silesian University of Technology, Faculty of Mechanical Engineering, Foundry Department, dawid.scelina@polsl.pl

<sup>4\*</sup>mgr Łukasz Bąk, Faculty of Transport, Silesian University of Technology, Department of Automotive Vehicle Service, lukasz.bak@polsl.pl

\* SWIFT - POKL.08.02.01-24-005/10

the creation of a group of materials : metal foams. Metallic foams are produced by metallurgical methods using appropriate blowing agent or blowing gas which forms bubbles (J. BANHART 2001, RUCHWA M. 2011). Because of their interesting characteristics and properties, metallic foams may serve as an alternative to the materials used in the automotive industry for example: the elements of the vehicle chassis, reducing the mass of the vehicle thereby enhancing its performance; in aerospace structural components for aircrafts. Due to porous structure metallic foams are very good at absorbing the kinetic energy and that makes them suitable for components with controlled deformation zone in the transport vehicles (J.W.H. KUMAR, P.D. HAYDN, N.G. WADLEY, Z. XUE 2008, A.G. EVANS, J.W. HUTCHINSON, M.F. ASHBY 1999, M. CHOLEWA 2003). Usage of metal foams as a replacement, however, is difficult due to the problem of joining them with other materials, different load distribution and different strength properties resulting from stochastic topography, ie randomness of the pore arrangement and stereological characteristics. These defects are not present in skeletal casts, for which by controlling the size and arrangement of joints it is possible to design the shape and size of cells. Skeleton castings manufacturing is based on the casting cores with prepared internal geometry using conventional casting methods (M. CHOLEWA, T.SZUTER, T. WRÓBEL, M. KONDRACKI 2012). The mechanical properties of these casts can be improved by using polymer filling materials, as confirmed by the initial studies conducted at the Department of Foundry, Silesian University of Technology (M. CHOLEWA. D. SCELINA 2011, 2012). The joint of the filling material with aluminum skeleton should give high adhesion and provide high strength properties, correctly distributing stress. Therefore, it is necessary to use materials which in the liquid state should dampen the surfaces, have low surface tension and after solidification form stable and strong adhesive joint. For further studies from duroplast materials chemically hardened epoxy resins were chosen, combining advantages of the technological and mechanical properties. Even in the case of complex compositions mainly

the epoxy resin – curatives rheological properties provoke skeleton reinforcement wetting processes. A significant influence on the dampening and adhesion of the preparation method has a surface which largely affects the strength of the joint. Effective development of area for aluminum alloys casting can be provided in a physical, chemical and electrochemical process. However, due to the geometric complexity of the skeleton casting skeletal casts and small areas between the surface of the developing ligaments usage of physical methods is difficult. It was therefore decided to increase the surface development of aluminum alloys by electrochemical oxidation. Coating produced by this method is porous and has a high surface development dependent on the chemical composition of the oxidized alloy (A. Posmyk 2010).

## **10.2. Conditions of the study**

The study attempted to determine the effects of inoculation of the structure causing fragmentation of  $\alpha$  solution of silicon in aluminum and the change of morphology and fragmentation of silicon ( $\beta$ ) at the assumed near-eutectic silicon content. For the AlSi11 alloy, the effects of inoculation on the oxidation process, topography of the oxidation surface as well as the thickness of the resulting oxide layer are described. The rationale for this research was the fact that, in the alloys of high silicon content in the process of anodizing may appear oxide layers with irregular structure and the isolated precipitates of alloying elements, especially silicon. From the technological point of view development of differentiated surface of the skeleton casting is most advantageous and desirable. In previous studies (M. CHOLEWA, D. SCELINA 2011) near-eutectic alloy of aluminum was selected, silicon AC-AlSi11 (Table 2.1) as a material for skeleton casting manufacturing. One of the important feature of the structure made from this alloy is the characteristic absorption of static and dynamic loads by partial plastic deformation and brittle fracture of spatial lattice ligaments. The proposed composition of the alloy and the characteristics of the microstructure can give

information about the behavior of plastic and brittle under-and over-eutectic alloys. An additional advantages of the chosen material are very good casting properties for such the complex geometry like skeleton castings where the diameter of ligament is about 5 mm.

**Table 10.1. Chemical constitution AlSi11 according to PN-EN 1706:2001**

Alloy	Chemical constitution, [%]								
	Si	Cu	Mg	Mn	Ni	Fe	Zn	Ti+Zr	Inne
<b>EN AC - AlSi11</b>	12,96	0,24	0,23	0,16	0,02	0,58	0,08	0,05	0,05

Source: Norm PN-EN 1706:2010

The scope of the study including the following:

- melting and metallurgical processing of alloy AlSi11;
- creating the experimental AlSi11 casts;
- electrolytic creations of the oxide layer with high surface area;
- thickness measurement and research were made with the use of Taylor-Hobson profilograph surface topography of the oxide layer;
- microscopic examination of the surface after oxidation;
- measurement of adhesion of the resin to the AlSi alloy.

### **10.2.1. Processing of metallurgical and casting AlSi alloy**

The melting and modification AlSi11 was performed in a graphite crucible placed in a laboratory induction furnace. For modification of AlSi11 alloy strontium content of 80 ppm was used. Pouring temperature of 670 ° C, to shell mould (silica sand / thermosetting resin) Test castings were machined to desired size (Fig. 10.1).



**Fig.10.1. Geometrical form of the samples used for testing.**

*Source: own study.*

### **10.2.2. Anodic oxidation of the samples**

The oxidation of the samples was done in a way that allowed to control the effect of the relation between cathode and ligament. It is important in shaping the oxide coating.

Therefore, the plating tank of the sample provided in a controlled way Fig. 10.2) which enables the oxide film thickness distribution depending on the position of the oxidized surface (5) relative to the cathode (6). In the tank there are two types of samples: having a square cross section (5) and round (3).

The arrangement of the square sample is directly related to the formation of an oxide layer, the fastest increase of the oxide layer is present on a surface that is closest to the cathode (areas I and II, Fig. 10.2).

This comes directly from the distribution of magnetic field lines. Figure 10.2 shows the circular sample (3), which is a model cross-sectional shape of the cells forming the connector skeleton casting.

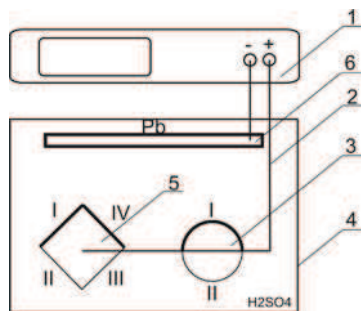


**Fig.10.2. The scheme of the anodic oxidation of samples from the spacing: 1 - power supply unit, 2 - power cords, 3 - oxidized sample (cylindrical), 4 - galvanic tank, 5 - oxidized sample (rectangular) connected to the positive terminal of the power supply (+) 6 - electrode lead - cathode (-).**

Source: own study.

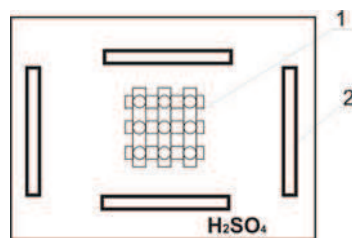


**Fig. 10.3 The scheme of the oxidation of real objects: 1 - cast skeleton connected to the positive pole of the power source - the anode (+), 2 - electrode lead cathode (-).**

Source: own study.

On the surface of the sample there are two indicated areas: I, which was expected to have a thicker coating and the area II, where the oxide film was expected to have a smaller thickness. The target orientation of skeleton casting relative to lead electrodes 4 (Fig.10.3) during the process of electrolysis there can be "shaded" areas, particularly the interior, in which one side is made thinner oxide layer. During the oxidation of samples one can use two lead electrodes and reduce differences in the thickness of the oxide coating, but during the oxidation

of the spatial lattice it is not possible to introduce the electrodes between ligaments. There is only the possibility of using multiple electrodes, as shown in Fig.10.3.

To study the influence of oxidation on the surface topography using two sets of samples made of the following materials: aluminum alloy with silicon (AC-AlSi11) and modified (mortar aluminum - strontium) aluminum-silicon alloy (Al<sub>i</sub>11 + M). For each of the groups 3 samples were created. Anodizing was carried out as follows:

- etching;
- sensitisation;
- anodized at a current density of 0.8 A dm<sup>2</sup>.

### 10.2.3. Measuring the thickness of the oxide layer

Measurement of thickness of the oxide layer on the surfaces of the samples was performed (Fig. 2.4) in the 10 selected points with the meter using eddy current (Fischeroskopu) measuring with an accuracy of 5% of the measured value.

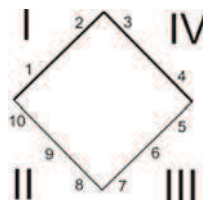


*Fig.10.4. Cross-section of the sample with the selected measurement points (1-10) oxide layer thickness.*

*Source: own study.*

### 10.2.4. Researches were made with the use of Taylor-Hobson profilometer surface topography

In order to determine the topography of the surface oxide coatings produced on the test AlSi alloy as tests were performed contact less, 3D

and 2D profilometer using optical profilometer Thanks to the device measurements without degradation and deformation of the silicon precipitates and coatings, which take place during the measurement method with contact.

### 10.2.5. Measurement of adhesion to the surface of the resin AlSi alloy

The samples were joined with the epoxy composition. Cross-linking of the resin was performed at room temperature for 24 hours. AlSi11/EP samples were tested for tensile strength.

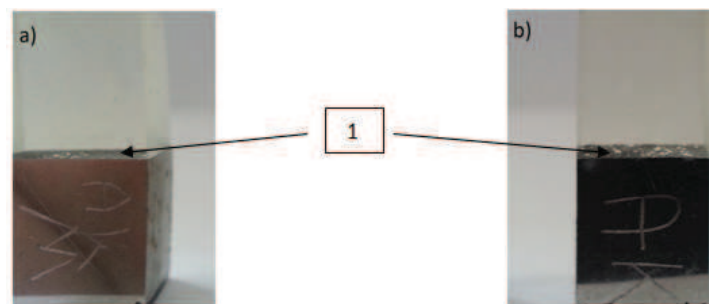


*Fig. 10.5. Adhesive connection area (1) Tensile strength test connector silumin-resin: a - AlSi11/EP, b - AlSi11 + M / EP.*

*Source: own study.*

## 10.3. The test results

### 10.3.1. The study of macro-and microscopic

Samples after oxidation were tested macroscopic, microscopic and profilometer to determine its topography. The results of macroscopic shown in Fig. 10.5, and the microscope in Fig. 10.6÷10.11.



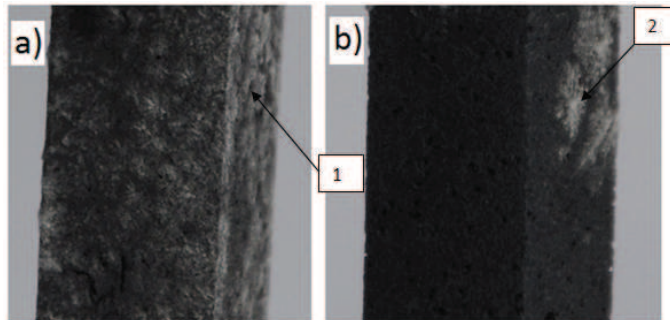


**Fig. 10.6.** View surface of the samples after oxidation: a) AlSi11, b) AlSi11 + M: 1 - oxide coating was thicker in place without silicon alloy non modified, 2 - oxide coating was of greater thickness at the silicon melt without modified.  
 Source: own study.

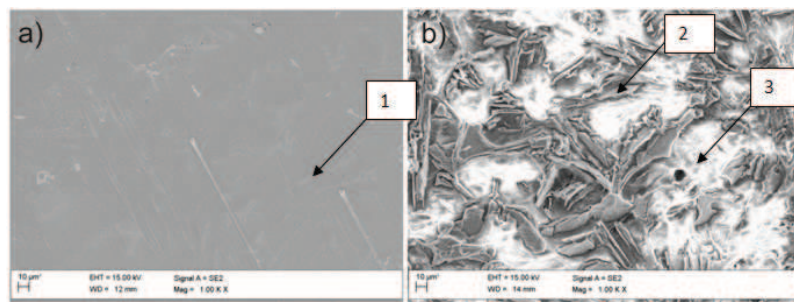


**Fig. 10.7.** View of AlSi11 alloy surface from oxidation (a) and after oxidation (b): 1 - educe silicon 2 - separation of silicon by chemical and electrochemical processing, 3 - oxide coating formed on the alloy  $\alpha$  solution.  
 Source: own study.

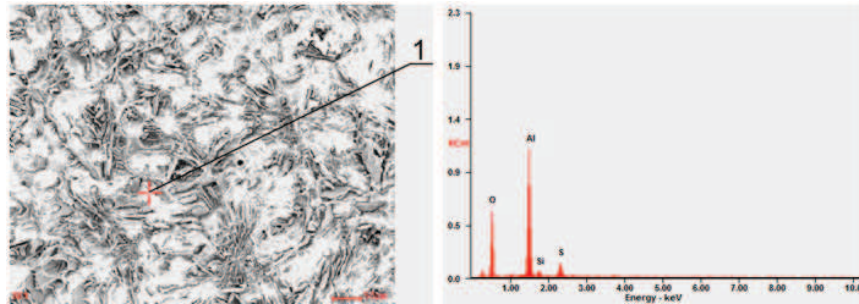


**Fig. 10.8.** View of of the surface of the alloy AlSi11 for qualitative analysis (a) and the content of selected elements (b): 1 - point analysis of the chemical constitution of the oxide coating.

Source: own study.

**Table 10.2.** Percentage content elements point analysis

Component	Wt%	At%
O	36,05	42,40
Al	39,28	27,39
Si	02,52	01,69
S	06,32	03,71

Source: own study.

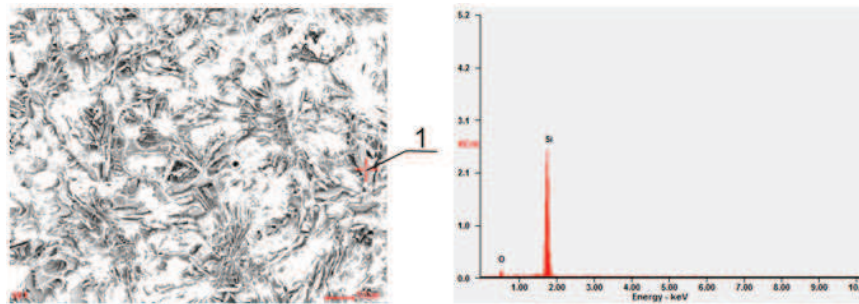


**Fig. 10.9.** View of of the surface of the alloy AlSi11 for qualitative analysis (a) and the content of selected elements (b): 1 - the point of analysis for the educe of the chemical constitution of silicon.

Source: own study.

*Table 10.3. Percentage content elements point analysis*

Component	Wt%	At%
O	09,83	16,06
Si	90,17	83,94

Source: own study.

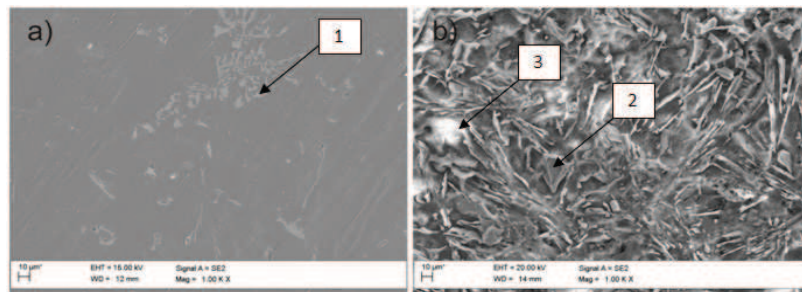


*Fig. 10.10. View of surface of the alloy AlSi11 + M before (a) and after oxidation (b): 1 - educe of silicon, 2 - educe the silicon exposed by the chemical or electrochemical processing, 3 - oxide coating on the alloy matrix.*

Source: own study.

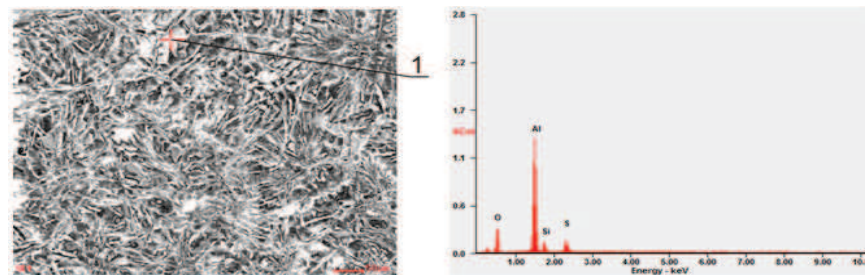


*Fig. 10.11. View of of the surface of the alloy AlSi11 + M for qualitative analysis (a) and the content of selected elements (b): 1 - point analysis of the chemical constitution of the oxide coating.*

Source: own study.

*Table 10.4. Percentage content elements point analysis*

Component	Wt%	At%
O	26,96	31,41
Al	40,22	27,78
Si	05,16	03,43
S	05,71	03,32

Source: own study.

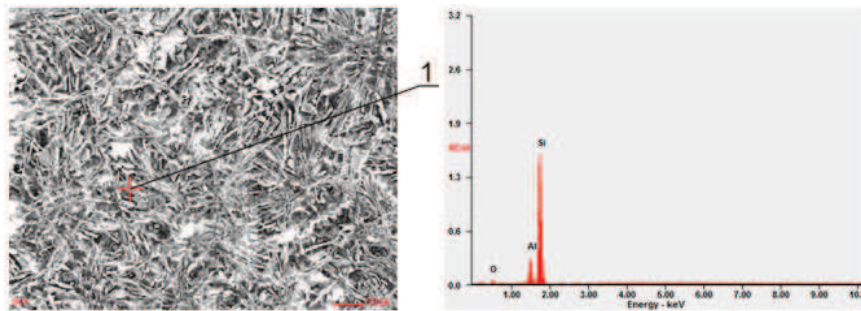


*Fig. 10.12. View of of the surface of the alloy AlSi11 + M for qualitative analysis (a) and the content of selected elements (b): 1 - the point of analysis for the educe of the chemical constitution of silicon.*

Source: own study.

*Table 10.5. Percentage content elements point analysis*

Component	Wt%	At%
O	07,19	11,91
Al	12,79	12,56
Si	80,02	75,52

Source: own study.

### 10.3.2. Measurement of coating thickness

The measurement results of oxide film thickness of the oxidized material at particular points (as shown in Fig. 10.4) depending on the position with respect to the cathode are shown in the form of bar graphs in Fig. 10.13-10.14, and their comparison in Fig. 10.15.

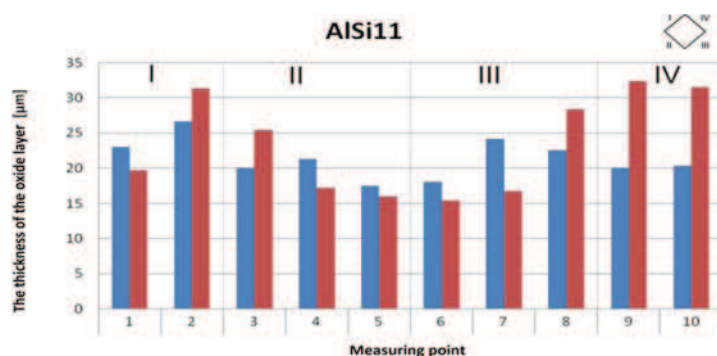


Fig. 10.13. Statement of oxide layer thickness of 10 measuring points for AISi11.

Source: own study.

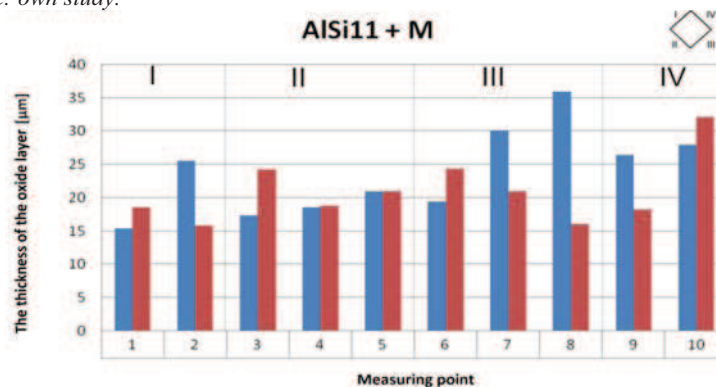
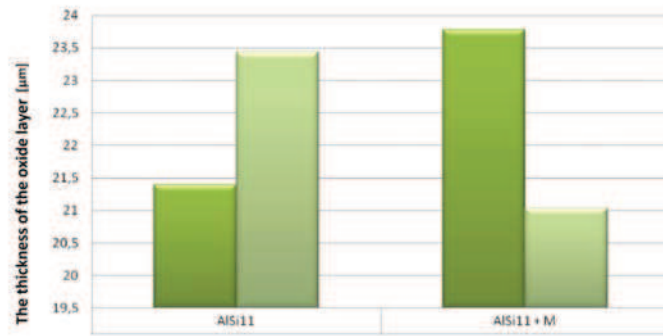


Fig. 10.14. Statement of oxide layer thickness of 10 measuring points for AISi11+M.

Source: own study.

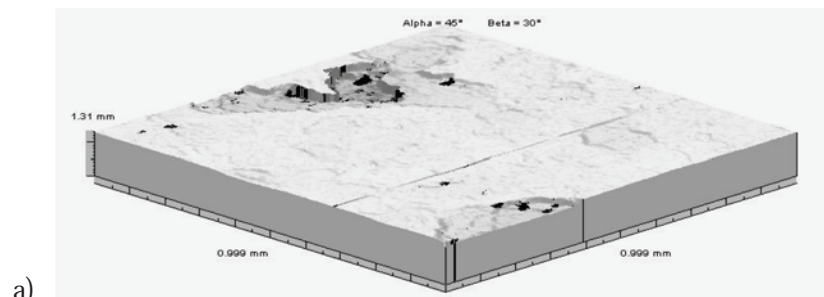


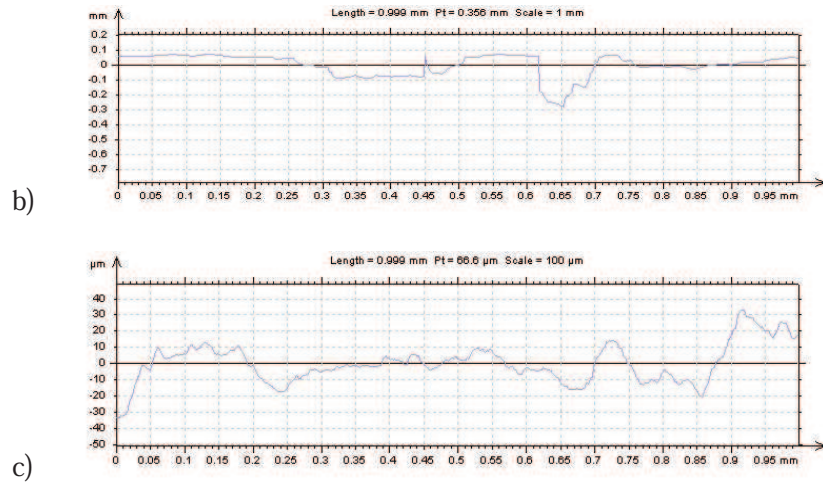
*Fig. 10.15. Comparison of the thickness of the oxide layer produced on the test materials.*

*Source: own study.*

### 10.3.3. Profilometer investigation

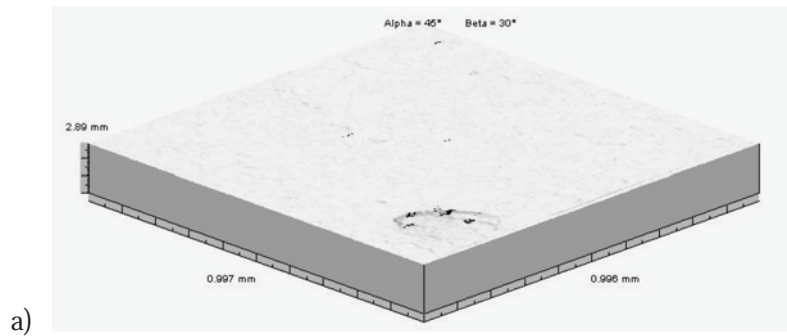
During the tests 3 profilometer 3D profiles (Figs 10.16a and 10.17a) and 2D (Figs 10.16b, c and 10.17b, c) were registered, which read the parameters in elevation summarized in Table 10.6.





**Fig. 10.16.** Influence of the oxidising process on the AlSi11 alloy surface topography: a) 3D-Roughness profile, b) 2D-Roughness profile from the place after Si-grain removing, c) 2D-Roughness profile from the flat surface.

Source: own study.





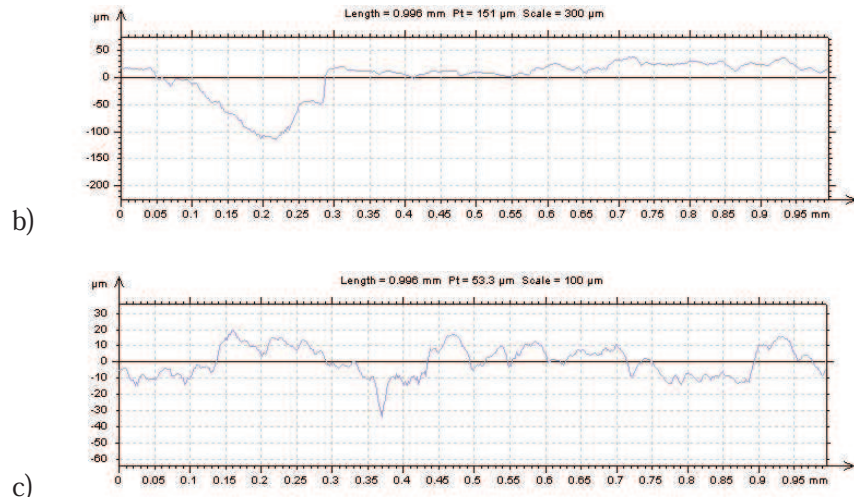


**Fig. 10.17.** Influence of the oxidising process on the AlSi11M alloy surface topography: a) 3D-Roughness profile, b) 2D-Roughness profile from the place after Si-grain removing, c) 2D-Roughness profile from the flat surface.

Source: own study.

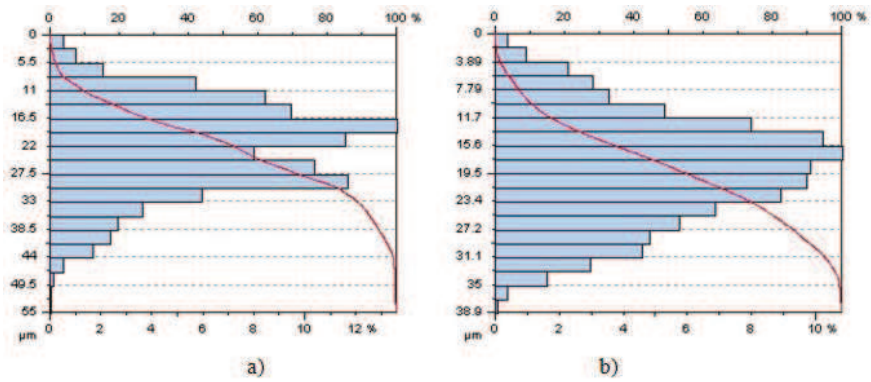


**Fig. 10.18.** Abbot-curves for surfaces of investigated alloys: a) AlSi11-alloy, b) AlSi11M-alloy.

Source: own study.



*Table 10.6. Chosen surface roughness parameters of anodic oxide layer on investigated alloys*

	Ra μm	Rp	Rv
AlSi11O <sup>1)</sup>	18,3	40	1270
AlSi11MO <sup>1)</sup>	6,85	19,8	21,8

<sup>1)</sup> oxidized

Source: own study.

#### 10.3.4. Measurement of adhesion of the resin to the oxidized surface AlSi alloy

During the study a series of breakaway strength tests of samples were taken from AlSi11/EP and AlSi11 + M / EP. The values of measured force at which the destruction of resin- AlSi alloy joint occurred allowed to determine damaging stress damage. The results are shown in Fig. 10.19.

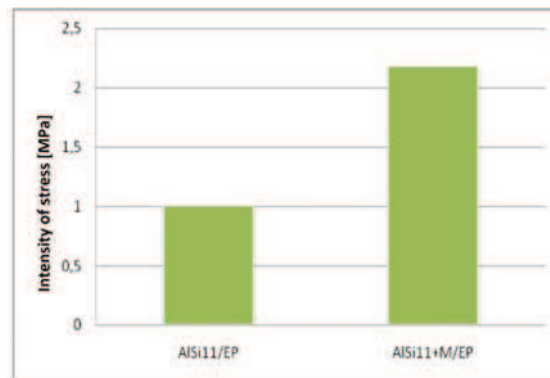


*Fig. 10.19. Summary of the results of breakaway strength of samples made of AlSi11/EP and AlSi11 + M / EP.*

Source: own study.

## 10.4. Discussion of the results

Microscopic analysis shows that the oxide film formed on the unmodified alloy AC-AlSi11 is discontinuous (Figs. 10.6÷10.9) and consists of a large number of large islets (3, 10.7b) separated by large Si precipitates (2, Figure 10.7b) which is confirmed by the results of the qualitative analyzes (Figs 2.8-2.9 and Table 10.4). The reason for this formation is the structure of the alloy, which consists of large Si precipitation (1, Fig. 10.7a) and larger areas of the matrix. Thicker layer is formed on the aluminium matrix.

The precipitation in the inoculated AlSi alloy are fragmented (1, Fig. 10.10a), and therefore there are larger number of them. Therefore, during the oxidation are formed small, few islets oxide coating (3, Fig. 10b) separated by a large amount of silicon precipitates (2, Fig 10.10b). This is confirmed by the results of qualitative analysis (Figs 10.11÷10..12 and Table 10.5).

From the analysis of the measurement results of oxide film thickness it is clear that the surfaces of the samples produced from the cathode coating have a thickness greater than at the opposite (Figs 10.13÷10..14), both the alloy and the unmodified or modified.

In the analysis of charts of surface roughness after oxidation test alloys that electrolytic oxidation process consisting of chemical and electrochemical oxidation has a significant impact on the topography of the surface alloy. Also the topography significantly affects AlSi alloy modification. In the unmodified alloy containing more grains of silicon, there is the leaching of chemicals, which is a consequence of larger craters (Fig. 10.16b: width up to 400  $\mu\text{m}$ , 400  $\mu\text{m}$  depth) of the produced oxide layer. The oxide formed on the foot modified smaller craters (Fig. 10.117b) with a depth of 100  $\mu\text{m}$  and a width of 250  $\mu\text{m}$ . Distribution of surface roughness at the vertices after oxidation AlSi alloy modified is closer to normal (Fig. 10.18) than unmodified. Area share of curves (solid line in Fig. 10.18) shows a large volume of cavities inequalities and helps to increase the adhesion of the resin to AlSi alloy.

By extending the surface as obtained by the anodic oxidation of the filler material of skeleton castings adhesion not only creates a joint in a place where there is an oxide layer, but on the exposed are anchored on precipitated silicon phase, which protrude above the surface. On the surface areas can also occur where the filler material flows into the large craters, which were created by the removal of silicon precipitates during chemical and electrochemical machining.

AlSi11 alloy inoculation treatment comminuted large hard phase precipitation of silicon during the oxidation which may be exposed and connected to the filler material can crumble even at low loads weakening the joint.

Color sample surface after oxidation (Fig. 10.4 b, c) for AlSi11 and AlSi11 + M is changed to black, it can provide the etching in the oxidation of aluminum and silicon unveiling phase precipitates in the samples (Fig. 10.4 c) AlSi11 + M appear brighter areas on the surface after oxidation, it may provide for the accumulation of Al<sub>2</sub>O<sub>3</sub> layer between the silicon phase precipitates, which was confirmed by quantitative analysis (Fig. 10.11÷10.12).

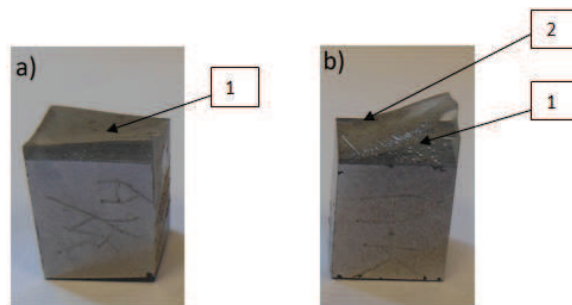


**Fig. 10.20. Image for connection with visible destruction zone for samples a) AlSi11 + M / EP, b) AlSi11/EP 1 - damage cohesive zone 2 - zone of destruction adhesive.**

*Source: own study.*

Strength of the samples is relatively low (Fig. 10.19), this follows from the fact that the resin, as compared to the alloy has a relatively low strength properties.

While test of the adhesion of the resin to the sample AlSi11 + M (Fig.10.20a) tensile strength increase led to a rupture of intermolecular bonds in epoxy resin composition, and thereby to decohesive destruction. On the surface destruction of the resin during adhesion tests to the sample AlSi11 (Fig.10.20b), two zones are shown ie the residue of the resin and the exposed surface of the oxide. It can be assumed that in the initial stage of destruction had decohesion character, resulting expanded area to the time when the increasing tension resulting from the reduction in surface area resulted in the accumulation of destructive stresses in the epoxy resin composition.

## 10.5. Summary

The study results showed a significant effect of electrolytic oxidation of the alloy casting AC-AlSi11 both unmodified and modified on the topography of the surface. Obtained oxide coating is the islet structure ie consists of a greater thickness formed on the material of the matrix and of a very small thickness formed around the silicon precipitates. Also the distance from the cathode surface affects the coating thickness and a uniformity of the structure, which have an impact on the adhesion of the resin. The shell is composed from a lot of craters that can be penetrated when filling with liquid resin. This was confirmed by strength tests. Surface topography of the oxide coating on the alloy samples AlSi11 + M has a different profile with protruding silicon fine precipitates which form in combination with the resin durable and strong joint. Modification resulting in fragmentation of AlSi alloy the silicon precipitates results, the coating has a more uniform structure, regardless of the position of oxidation surfaces relative to the cathode.

Despite the known adverse effects on the border of epoxy - aluminum alloy obtained favorable combination of aluminum alloy with an epoxy

resin, as evidenced by the prevalence of cohesive mechanism of destruction compared to the mechanism of joint destruction adhesive materials.

### **Bibliography**

1. M. Cholewa, D. Scelina, A. Dulęba 2011. *Call adhesive in casting composites epoxy resin/AlSi*, Polimery i kompozyty konstrukcyjne.
2. M. Cholewa, D. Scelina, A. Dulęba 2012. *Wytrzymałość na ściskanie Kompozytów AlSi 11/ beton z polimerem siarkowym*. Przetwórstwo tworzyw 6(146). str. 174 – 178.
3. M. Cholewa 2003. *Spatial, composite foam castings*, Archives of Foundry 3/9 81-88 (in Polish).
4. M.Cholewa, T.Szuter, T.Wróbel, M.Kondracki 2012. *The skeleton castings as a new type of cast lattice structures*, Journal of Achievements in Materials and Manufacturing Engineering 54/2 250-259
5. 5 Ruchwa M. 2011. *Analiza elementów konstrukcyjnych wykonanych ze spienionych metali*, Materiały Budowlane, 10
6. Posmyk A. 2010. *Surface layers on aluminium engineering alloys*. Publ. of SilesianUniversity of Technology. ISBN 978-83-7335-764-8
7. J.W.H. Kumar, P.D. Haydn, N.G. Wadley, Z. Xue 2008. *Mechanical response of metallic honeycomb sandwich panel structures to high-intensity dynamic loading*, International Journal of Impact Engineering 35/9 1063-1074.
8. A.G. Evans, J.W. Hutchinson, M.F. Ashby 1999. *Multifunctionality of cellular metal systems*, Progress in Materials Science 43 171-221.
9. J. Banhart 2001. *Manufacture, characterisation and application of cellular metals and metal foams*, Progress in Materials Science 46/6 559-632.